RSC Advances

ROYAL SOCIETY OF CHEMISTRY

www.rsc.org/advances

Title: Preparation of biocompatible and antibacterial carbon quantum dots derived from resorcinol and formaldehyde spheres

Authors: Arup Kumer Roy, Sung-Min Kim, Peerasak Paoprasert, Sung-Young Park and Insik In

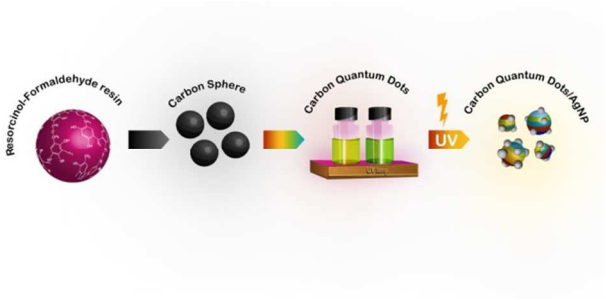

RSC Advances

RSCPublishing

ARTICLE

Preparation of biocompatible and antibacterial carbon quantum dots derived from resorcinol and formaldehyde spheres

Cite this: DOI: 10.1039/x0xx00000x

Arup Kumer Roy,[a] Sung-Min Kim,[b] Peerasak Paoprasert,[c] Sung-Young Park,[b,d*] and Insik In[a,d*]

Received 00th January 2012,
Accepted 00th January 2012

DOI: 10.1039/x0xx00000x

www.rsc.org/

Green or yellow emitting carbon quantum dots (CQDs) were prepared through the combination of bottom-up and top-down approaches from resorcinol and formaldehyde. The prepared CQDs showed characteristic fluorescence behavior depending on the compositional or structural features. Both CQD-S (green emitting) and CQD-P (yellow-emitting) were physiologically stable and biocompatible as cancer cell bioimaging agents. Especially, silver nanoparticle (Ag NP)-decorated CQDs revealed very good antibacterial activity for Gram-positive *S. aureus* and Gram-negative *E. coli*.

Introduction:

Recently, carbon quantum dots (CQDs) have been intensively researched as the next generation carbon nanomaterials in addition to OD fullerene, 1D carbon nanotube and 2D graphene. CQD's promising optoelectrical properties are approaching or jumping to those of counterparts, inorganic quantum dots (QDs). CQDs have been widely examined in various applications such as bioimaging,[1-4] sensing,[5,6] photo/electrocatalysis,[7] light-harvesting,[8] and drug-delivery systems[9,10] through the exploitation their biocompatibility, low toxicity, excellent photochemical stability and facile surface functionalization.

Up to now, two different categories of approaches, "top-down" and "bottom-up" approaches have been typically adopted for the synthesis of CQDs depending on the type of source or precursor materials.[11] In "top-down" approach, carbon nanomaterials with well-defined morphology such as carbon nanotubes,[12] nanodiamonds,[13] graphene oxide,[14] graphite[15] and carbon fiber,[16] together with carbon-rich materials with less-defined morphology such as carbon soot,[17,18] activated carbon,[19] carbon black[20] and paper ash[21] have been able to be broken down to CQDs with high dispersion stability and tuneable fluorescence emissions through discharge,[22] laser ablation[23] and chemical/electrochemical oxidation.[12] In "bottom-up" approach, various small molecules, polymers and even biocompatible materials have been utilized for the synthesis of CQDs through combustion, thermal treatment, thermal/chemical carbonization, electrochemical and acid/alkali-assisted ultrasonic or oxidation reactions. CQDs prepared by "bottom-up" approach have been successfully utilized for the applications such as sensing and bioimaging with or without surface passivation to enhance the quantum yield and brightness of CQD fluorescence. While "bottom-up" approach using "green" precursors is much more preferable to the bioapplications of CQD where the physiological stability of material is required, "top-down" approach using carbon-rich materials is much more feasible for defining of expected structural/compositional/optoelectrical features of the resulting CQDs. Additionally, the carbon-rich materials show consistent structures and compositions regardless of the supply while "green" precursors show significant variation depending on the source. Therefore, another synthetic approach combining the advantages of both "bottom-up" and "top-down" approaches could be versatile for the preparation of CQDs with precise controlled optoelectrical properties, reproducibility, and scalability.[24] In our method, resorcinol and formaldehyde that are cheap and extensively consuming as the monomers for the production of resorcinol-formaldehyde (RF) resin in industry were used as the starting materials for the synthesis of RF-based CQDs having two different sizes and fluorescence emission color (green and yellow) with the quantum yield up to 1%. The prepared CQDs were used safely for in vitro imaging of A549 human lung cancer cells through the virtue of non-cytotoxicity of CQDs. In addition, highly anti-bacterial CQDs

toward both *Staphylococcus aureus* (gram positive) and *Escherichia coli* (gram negative) were simply prepared by electroless silver deposition on CQDs through the exploitation of rich oxygen functionalities of the surface of CQDs.[25] Other important feature of RF-based CQD is its scalability for the mass production and grams of CQDs were reproducibly obtained from each reaction.

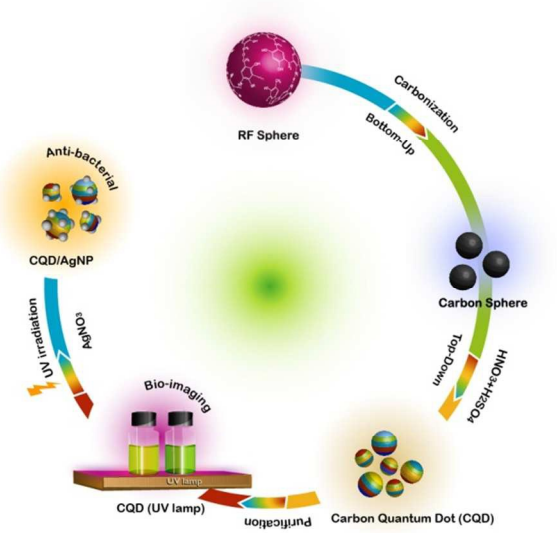

Scheme 1. Schematic illustration for the overall synthetic procedure of CQD and CQD/Ag NP.

Experimental:

Materials and Characterization

Resorcinol (C_6H_4-1,3-$(OH)_2$, ≥ 99.0%), formaldehyde (HCHO, 37%) solution, ammonium hydroxide (NH_4OH, 28-30%), ethanol (C_2H_5OH, ≥ 99.5%), silver nitrate ($AgNO_3$, ≥ 99.0%), Pluronic F127 (Mw: 12,600 Da), sodium carbonate (Na_2CO_3) were purchased from Sigma-Aldrich and sulfuric acid (H_2SO_4, 95%), nitric acid (HNO_3, 60%) were purchased from Samchun Chemicals, South Korea. All chemicals were used without further purification step.

Fourier transform infra-red (FT-IR) spectra were acquired on a Nicolet iS10 FT-IR spectrometer (Thermo Scientific). Atomic force microscopy (AFM) images were acquired by Multimode-N3-AM nanoscope 3D scanning probe microscopy (SPM) system (Bruker). Field emission scanning electron microscopy (FE-SEM) images were obtained by JSM-6700F FE-SEM (JEOL). Ultraviolet-visible (UV-Vis) spectra were measured by Optizen α UV-Vis spectrometer (Mecasys, South Korea). The luminescence properties were examined by using a fluorescence spectrometer (SCINCO, FS-2, South Korea) with a xenon lamp excitation source (150 W). The X-ray diffraction (XRD) measurements of the powder samples were recorded on a Bruker D8-Advance X-ray powder diffractometer using Cu Kα radiation (λ=1.5406 Å). X-ray photoelectron spectroscopy (XPS) spectrum was recorded with a Thermo VG Scientific Sigma Probe spectrometer. Transmission electron microscopy (TEM) images were taken on a TECNAI F20 (Philips) at 200 kV. Raman spectroscopy measurements were performed on a ARAMIS Raman spectrometer (Horiba Jobin Yvon, France) by using 514.5 nm laser radiation. Helios 06 (15W) double side vacuum exposure unit (South Korea) used for UV-Vis irradiation.

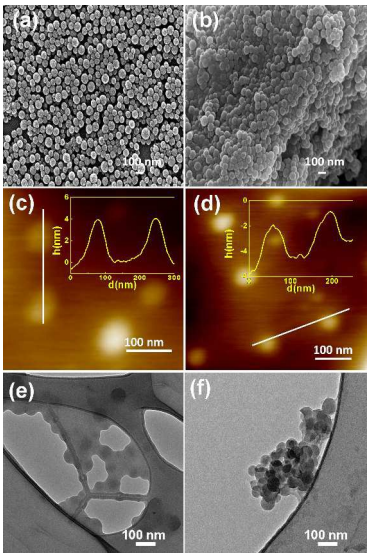

Fig. 1 SEM images of (a) RF (b) CS, AFM and TEM images of (c), (e) CQD-S and (d), (f) CQD-P respectively.

Preparation of Carbon spheres (CS) from resorcinol and formaldehyde (RF)

At first, spherical RF nanoparticles (RF NPs) with diameter of about 100 nm were prepared by using condensation reaction of resorcinol and formaldehyde as monomers through a modified Stöber method using Pluronic F127 as a stabilizer in alcohol/water medium. In brief, at first, 0.4 ml of aqueous NH_4OH solution was mixed with 32 ml of absolute ethanol and 80 mL of deionized water (H_2O) under vigorous stirring for 1h. After then, resorcinol (0.8 g) and Pluronic F127 (1.69 g) was added into the solution with continually stirring for 30 min. Then, formaldehyde solution (1.12 mL) was added to the reaction mixture and stirred for 24 hrs at 30 °C and subsequently heated for 24 hrs at 100 °C under a static condition in a Teflon-lined autoclave. The solid product was recovered by centrifugation and freeze-dried for 48 hrs. At second, thermal treatment of RF NPs between 350 °C for 2 hrs and 600 °C for 4 hrs (1°/min) under nitrogen atmosphere provided black powders of carbon sphere (CS) NPs showing 67.1% decrease of weight due to the dehydration and carbonization during thermal treatment process.[26]

Synthesis of CQD-S and CQD-P

50 mg of CS NP powder was treated with the mixture of sulfuric acid and nitric acid (volume ratio of 1:2) and the reaction mixture was heated at 100 °C for 12 hrs in a Teflon-lined autoclave after brief sonication in bath sonicator for 3 hrs

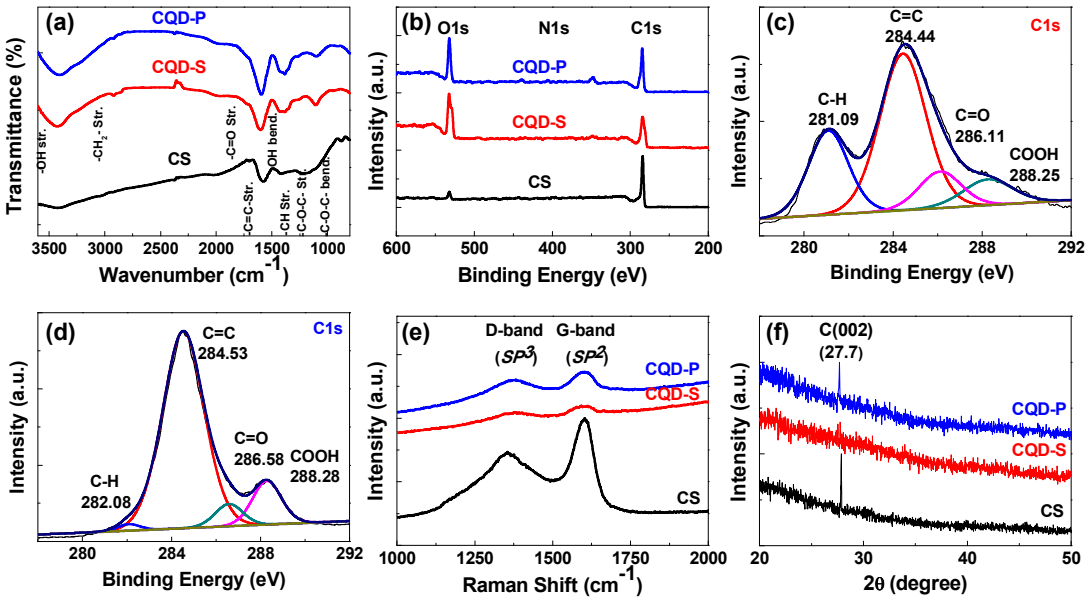

Fig. 2 (a) FT-IR spectra, (b) XPS full survey scans, deconvoluted C1s peaks of (c) CQD-S and (d) CQD-P, (e) Raman spectra (excited with 514.5 nm laser) and (f) XRD profiles of all the samples [Cu Kα radiation (λ=1.5406 Å)].

at room temperature. After acid treatment, most of CS powders were dissolved into the acid medium and highly transparent red-colored CQD solution was obtained after dilution with water with little noticeable floating particles. The selective isolation of RF-based CQDs with different fluorescence color was attempted by controlled ultracentrifuge of the crude CQD solution. After ultracentrifugation for 20 min at 4,000 rpm, red-colored supernatant solution (CQD-S) and dark brown precipitated (CQD-P) were separately divided and stored. To remove acid residue from RF-based CQDs, dialysis of CQD solutions were attempted by using molecular weight cut-off membrane (MWCO 1,000 Da) for 72 hrs. Finally, 3 and 6 mg of CQD-S and CQD-P were obtained after freeze-drying of each dialyzed CQD solution, respectively.

Synthesis of Ag NP decorated CQDs

In a typical preparation, 1.5 ml of $AgNO_3$ solution (1 mM) and 1.5 ml of aqueous solution of CQD were mixed with vigorous stirring. Then, the mixture solution was irradiated with UV lamp for 40-45 min. After the irradiation, the initially pale-brown solution turned to dark-yellow solution, presenting the UV-assisted reduction of Ag^+ ions to AgNPs. Solid Ag NP decorated CQD was collected by centrifugation (12000 rpm, 1 hr) and subsequent freeze-drying.

Results and discussion

Both "bottom-up" and "top-down" approaches are sequentially attempted to provide RF-based CQDs from RF. The overall synthetic procedure is illustrated in Scheme 1.

In fig. S1, while CS was only soluble in isopropyl alcohol, ethanol and tetrahydrofuran, both CQDs were soluble only in water probably due to the rich oxygen functionalities on their surface. The formation of CQDs from RF was firstly confirmed with scanning electron microscopy (SEM), transmission electron microscopy (TEM) and atomic force microscopy (AFM) analysis. While both the spherical shape and size distribution of RF NPs were preserved after carbonization to CS NPs, the SEM images of RF NPs and CS NPs showed the sight volume shrinkage after carbonization process from 100±20 nm to 90±10 nm (Fig. 1a,b). The AFM images of CQD-S and CQD-P showed that RF-based CQDs have carbon dot-like morphologies. While both CQDs showed particle diameters of 40±0.5 and 50±1.0 nm, respectively, the thickness was about 4 nm in both CQDs (Fig 1c,d). Therefore, it is regarded that RF-based CQDs have anisotropic 2D disc-like morphology. Considering that typical CQDs obtained from other top-down approaches shows dot-like morphology with the particle size less than 10 nm, the disc-like morphology of RF-based CQDs are very unique. Only few studies have reported the preparation of CQDs with similar disc-like morphology through top-down approach from either single-walled carbon nanotube (SWNT) or pitch-based carbon fiber (CF) which has rich sp^2 carbon content. The TEM images of RF-based CQDs showed that both CQDs have similar lateral dimensions of between 40 and 50 nm, which is corresponding to the previous AFM analysis (Fig. 1e,f).

Further compositional and structural features of RF-based CQDs were examined by Fourier transform infrared spectroscopy (FT-IR), X-ray photoelectron spectroscopy (XPS), Raman spectroscopy and X-ray diffraction (XRD) analysis. The FT-IR spectra of both CQDs showed that RF-based CQDs have rich oxygen functionalities such as hydroxy (-OH) and carboxylic acid (COOH) groups together with aromatic backbone (Fig. 2a). Both CQDs revealed the occurrence of significant carboxylic acid stretching peaks at around 1,720 cm^{-1}, which was not observable in CS NP.

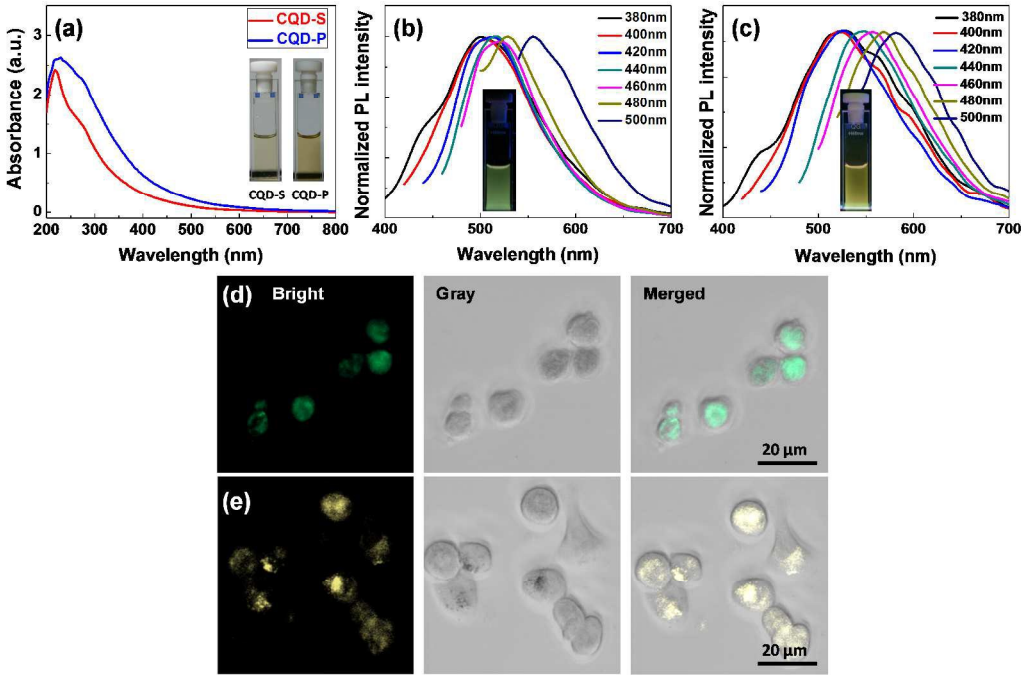

Fig. 3 (a) UV-Vis spectra (insets are photo images of CQD solutions with concentration of 0.25 mg/mL) and normalized fluorescence spectra of (b) CQD-S, (c) CQD-P at different excitation wavelengths (insets are photo images of CQD solutions with excitation of 365 nm UV), confocal microscopy images (488 nm light excitation) of A549 cells incubated with (d) CQD-S, (e) CQD-P.

Interestingly, aromatic C=C stretching peak of CS NP at 1,576 cm^{-1} was significantly shifted to 1,594 and 1,600 cm^{-1}, respectively, in the case of CQD-S and CQD-P. Both CQDs revealed the strong -OH stretching peaks at 3,410 cm^{-1} and CS NP showed only weak signal in this region. More detailed compositional information of RF-based CQDs was obtained from XPS analysis (Fig. 2b). The three peaks observed at 284.0, 401.0 and 533 eV are considered as C1s, N1s and O1s binding peak, respectively. While CS NP showed carbon-dominant composition (C 93.2%, O 5.6%, N 1.2%), RF- based CQDs presented increased oxygen content more than 27%. CQD-S showed slightly higher inclusion of oxygen (C 63.3%, O 35.6%, N 1.0%) compared with CQD-P (C 71.0%, O 27.1%, N 1.8%). This higher oxygen content of CQD-S compared with CQD-P explains the higher dispersion stability of CQD-S during the centrifugation step because there is little structural inconsistency between them as confirmed from the previous discussions of AFM and TEM analysis. Deconvoluting C1s peaks of both CQDs showed the presence of significant oxygenated carbons. Four overlapping peaks 281.09, 284.44, 286.11 and 288.25 eV for CQD-S and 282.08, 284.53, 286.58, 288.28 eV for CQD-P indicate C1s peaks of C-H, C=C, C=O and COOH groups of CQDs, respectively. It is clear that the peak intensities of oxygen functionalities (OH, C=O and COOH) are much higher compared with pristine CS NP (Fig. 2c,d). Raman spectra of CS NP and CQDs were compared each other (Fig. 2e). Both showed characteristic D and G band peaks, which support the presence of significant sp^2 carbons (G band) together with sp^3 detects (D band) both in CS NP and RF-based CQDs. The D band to G band intensity ratio (I_D/I_G) was significantly increased after the formation of CQDs (0.90) from CS NP (0.74), from which we can assume that the observed structural defects might be introduced into CQDs by varying forms of oxygen functionalities including carbonyl, carboxyl, hydroxyl and epoxy groups into the sp^2 carbon skeletal of CS NP after the acid treatment. Interestingly, D band peaks of CQD-S and CQD-P were significantly shifted to 1,381 and 1,382 cm^{-1}, respectively, from 1,356 cm^{-1} in the case of CS NP while G band peaks didn't show remarkable shift from 1,600 cm^{-1}.[27a] While the origin of this low-frequency D band peak shift of RF-based CQDs is not clear in this stage, it is believed that the oxygen rich environments near the sp^3 defect sites of CQDs compared with carbon rich environment of CS NP might contribute to this shift. Then, crystalline structures of both CS NP and CQDs were exploited by XRD analysis (Fig. 2f). Pristine CS NP showed a sharp graphitic diffraction peak (002) at 2θ of 27.7° (d=3.22Å), which indicates the preservation of partial graphitic structure in CS NP. This graphitic scattering peak of CS NP was significantly diminished in CQD-S and preserved in CQD-P, respectively. This different crystallinity of CQD-S compared with CQD-P might come from the much highly oxygenated compositional feature of CQD-S.

Quasi 2D disk-like morphology of RF-based CQDs and their rich oxygen functionalities prompts us to investigate the optical properties of CQDs and their application toward cell imaging based on fluorescence. Ultraviolet-visible (UV-Vis) absorption spectra of CQD-S and CQD-P exhibited two strong absorption peaks at 220 and 229 nm, which are attributed to the π-π* transition peaks of the isolated sp^2 conjugated domains in

CQDs together with the overlapping peaks at 280 nm, which are attributed to n-π* transition peaks of the carbonyl (C=O) groups in CQDs (Fig. 3a).[27] With the excitation at 460 nm, CQD-S and CQD-P showed definitively green and yellow emission, respectively. Then, fluorescence spectra of both CQDs were examined in varying excitation wavelength from 380 to 500 nm (Fig. 3b,c). The normalized fluorescence spectra of CQD-S definitely showed maximum fluorescence emission between 501 and 555 nm (greenish emission), while CQD-P showed maximum fluorescence emission between 523 and 581 nm (yellowish emission). Any up conversion fluorescence was not observed in both CQDs. Above multicolour emissions of RF-based CQDs are typical features of CQDs whose fluorescence emission mechanism is based not on the band gap transition of conjugated π domains but on the surface defect-derived origin. The presence of different particle sizes of CQDs and different emissive trap sites in CQDs might contribute to the above tunable fluorescence emissions of RF-based CQDs. RF-based CQDs showed very good biocompatibility as cancer cell imaging agents. After the incubation of A549 lung cancer cells with CQDs for 24 hrs, most A549 cells were completely labeled with either green-emitting CQD-S or yellow-emitting CQD-P (Fig. 3d, e). Otherwise, MTT-mediated cell viability assay demonstrated more than 92% in the concentration range of 0-0.1 mg/mL, revealing the strong candidate for biological applications as non-toxic materials (Fig. S2). These results promoted as strong candidates to use in cellular imaging for diagnosis purposes.

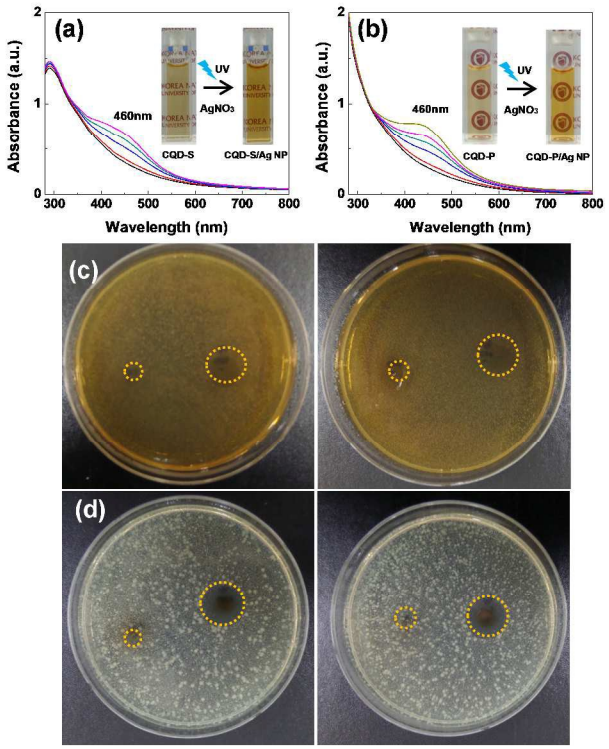

Fig. 4 UV-Vis spectra and schematic illustration of (a) CQD-S/Ag NP and (b) CQD-P/Ag NP before and after UV-irradiation. Antimicrobial activities of as prepared sample against (c) Gram positive S. aureus and (d) Gram negative *E. coli.*

Further hybridization of RF-based CQDs with silver nanoparticles (Ag NPs) was attempted by exploiting the rich oxygen functionalities on the surface of CQDs. Addition of silver nitrate ($AgNO_3$) into the aqueous dispersion of either CQD-S or CQD-P and the subsequent irradiation with UV light (365 nm) induced the growth of Ag NPs on RF-based CQDs within 1 hr. UV-Vis spectra of Ag NP-decorated CQD solutions clearly showed the surface plasmon resonance (SPR) peaks of Ag NPs at 460 nm (Fig. 4a,b). TEM and energy dissipate X-ray (EDX) analysis clearly revealed the presence of several Ag NPs on CQDs (Fig.S3). It is reported that the photo-excited electrons from CQDs enable the reduction of Ag^+ ions on the surface of CQDs.[25] XPS spectrum of Ag NP-decorated CQDs clearly showed the incorporation of significant Ag atoms (Fig.S4, S5). The presence of Ag NPs on RF-based CQDs presented very good antimicrobial activities for two model bacteria, Gram-positive *S. aureus* and Gram-negative *E. coli.*[28,29] Clear inhibition zones were observed after incubation of above model bacteria only with Ag NP-decorated CQDs, confirming the prevention both Gram-negative and Gram-positive bacterial growth (Fig. 3c, d).

Conclusion:

In summary, green or yellow emitting CQDs were prepared through the combination of bottom-up and top-down approaches from RF resin. The prepared CQDs showed characteristic fluorescence behavior depending on the compositional or structural features. Both CQD-S (green emitting) and CQD-P (yellow-emitting) were physiologically stable and biocompatible as cancer cell bioimaging agents. Especially, Ag NP-decorated CQDs revealed very good antibacterial activity for Gram-positive *S. aureus* and Gram-negative *E. coli*. Through the combination of both bottom-up and top-down approaches, CQDs with precise controlled optoelectrical properties, reproducibility, scalability applicable for both bioimaging and antibacterial agents were simply obtained from resorcinol and formaldehyde, cheap commodity chemicals. Further control of the size distribution of RF-based CQDs, the enhancement of fluorescence intensity through the surface passivation and the hybridization of RF-CQDs with other nanomaterials to accomplish the preparation of multi-functional CQDs is on-going.

Acknowledgement

This research was supported by Basic Science Research Program through the National Research Foundation of Korea (NRF) funded by the Ministry of Education (No. 2014055946), a grant from the Fundamental R&D Program for Core Technology of Materials funded by the Ministry of Knowledge Economy, Republic of Korea (1415120175), and Chungcheong Institute for Regional Program Evaluation (CIRPE) Promotion Project of the MOTIE (Ministry of Trade, Industry and Energy) Republic of Korea (A004600100).

Notes and references

[a]Department of Polymer Science and Engineering, Korea National University of Transportation, Chungju 380-702, South Korea.
[b]Department of Chemical and Biological Engineering, Korea National University of Transportation, Chungju 380-702, South Korea.
[c]Department of Chemistry, Faculty of Science and Technology, Thammasat University, Pathumthani 12121, Thailand.
[d]Department of IT Convergence (Brain Korea PLUS 21), Korea National University of Transportation, Chungju 380-702, South Korea.

†Electronic Supplementary Information (ESI) available: detail experimental procedure of *in vitro* and antibacterial activity, solubility test of CS, TEM images, EDX , Full and deconvoluting C1s, O1s, N1s and Ag3d XPS spectra of CQD-S/AgNP and CQD-P/AgNP. See DOI: 10.1039/c000000x/

1 L. Cao, X. Wang, M. J. Meziani, F. Lu, H. Wang, P. G. Luo, Y. Lin, B. A. Harruff, L. M. Veca, D. Murray, S. Y. Xie and Y. P. Sun, *J. Am. Chem. Soc.,* 2007, **129**, 11318-11319.
2 Z. A. Qiao, Y. Wang, Y. Gao, H. Li, T. Dai, Y. Liu and Q. Huo, *Chem. Commun*., 2010, **46**, 8812-8814.
3 C. J. Jeong, A. K. Roy, S. H. Kim, J. E. Lee, J. H. Jeong, I. In and S. Y. Park, *Nanoscale,* 2014, **6**, 15196-15202.
4 Z. Q. Xu, L.Y. Yang, X. Y. Fan, J. C. Jin, J. Mei, W. Peng, F. L. Jiang, Q. Xiao and Y. Liu, *Carbon*, 2014, **66**, 351-360.
5 C. Ding, A. Zhu, and Y. Tian, *Acc. Chem. Res*., 2014, **47**, 20-30.
6 M. Algarra, B. B. Campos, K. Radotic, D. Mutavdzic, T. Bandosz, J. J. Jimenez, E. R. Castellon and J. C. G. E. D. Silva, *J. Mater. Chem. A*, 2014, **2**, 8342-8351.
7 P. Mirtchev, E. J. Henderson, N. Soheilnia, C. M. Yip and G. A. Ozin, *J. Mater. Chem.,* 2012, **22**, 1265-1269.
8 X. Zhang, Y. Zhang, Y. Wang, S. Kalytchuk, S.V. Kershaw, Y. Wang, P. Wang, T. Zhang, Y. Zhao, H. Zhang, T. Cui, Y. Wang, Jun Zhao, W. W. Yu and A. L. Rogach, *ACS Nano*, 2013,**7**, 11234-11241.
9 S. Pandey, M. Thakur, A. Mewada, D. Anjarlekar, N. Mishra and M. Sharon, *J. Mater. Chem. B*, 2013, **1**, 4972-4982;
10 Q. Wang, X. Huang, Y. Long, X. Wang, H. Zhang, R. Zhu, L. Liang, P. Teng and H. Zheng, *Carbon*, 2013, **59** , 192-199.
11 S. Y. Lim, W. Shen and Z. Gao, *Chem. Soc. Rev.,* 2015, **44**, 362-381.
12 J. G. Zhou, C. Booker, R. R. Li, X. T. Zhou, T. K. Sham, X. L. Sun and Z. F. Ding, *J. Am. Chem. Soc*., 2007, **129**, 744-745.
13 S. J. Yu, M.W. Kang, H. C. Chang, K. M. Chen and Y. C. Yu, *J. Am. Chem. Soc*., 2005, **127**, 17604-17605.
14 Q. L. Wang, H. Z. Zheng, Y. J. Long, L. Y. Zhang, M. Gao and W. J. Bai, *Carbon*, 2011, **49**, 3134-3140.
15 Q. L. Zhao, Z. L. Zhang, B. H. Huang, J. Peng, M. Zhang and D. W. Pang, *Chem. Commun*., 2008, **0**, 5116-5118.
16 J. Peng, W. Gao, B.K. Gupta, Z. Liu, R. R. Aburto, L.Ge, L. Song, L. B. Alemany, X. Zhan, G. Gao, S.A. Vithayathil, B. A. Kaipparettu, A. A. Marti, T.Hayashi, J. J. Zhu and P. M. Ajayan, *Nano Lett.*, 2012, **12**, 844-849.
17 S. C. Ray, A. Saha, N. R. Jana and R. Sarkar, *Phys. Chem.* C, 2009, **113**,18546-1855.
18 H. P. Liu, T. Ye and C. D. Mao, *Angew. Chem., Int. Ed.,* 2007, **46**, 6473-6475.
19 Y. Dong, N. Zhou, X. Lin, J. Lin, Y. Chi and G. Chen, *Chem. Mater.* 2010, **22**, 5895-5899.
20 C. C. Wang and S. Y. Lu, *Nanoscale*, 2015, **7**, 1209-1215.
21 J. Wei, J. Shen, X. Zhang, S. Guo, J. Pan, X. Hou, H. Zhang, L. Wang and B. Feng, *RSC Adv.*, 2013, **3**, 13119-13122.
22 X. Xu, R. Ray, Y. Gu, H. J. Ploehn, L. Gearheart, K. Raker and W. A. Scrivens, *J. Am. Chem. Soc.,* 2004, **126**, 12736-12737.
23 Y. P. Sun, B. Zhou, Y. Lin, W. Wang, K. A. S. Fernando, P. Pathak, M. J. Meziani, B. A. Harruff, X. Wang, H. Wang, P. G. Luo, H. Yang, M. E. Kose, B. Chen, L. M. Veca and S.Y. Xie, *J. Am. Chem. Soc.* 2006, **128**, 7756-7757.
24 B. Zhu, S. Sun, Y. Wang, S. Deng, G. Qian, M. Wang and A. Hu, *J. Mater. Chem. C*, 2013, **1**, 580-586.
25 H. Choi, S. J. Ko, Y. Choi, P. Joo, T. Kim, B. R. Lee, J.W. Jung, H. J. Choi, M. Cha, J. R. Jeong, I.W. Hwang, M. H. Song, B. S. Kim and J.Y. Kim, *Nature Photon.*, 2013, **7**, 732-738.
26 J. Liu, S. Z. Qiao, H. Liu, J. Chen, A. Orpe, D. Zhao and G. Q. (Max) Lu, *Angew. Chem. Int. Ed*., 2011, **50**, 5947-5951.
27 J. Deng, Q. Lu, N. Mi, H. Li, M. Liu, M. Xu, L. Tan, Q. Xie, Y. Zhang and S. Yao, *Chem. Eur. J.,* 2014, **20**, 4993 - 4999.
28 A. K. Roy, B. Park, K. S. Lee, S. Y. Park and I. In, *Nanotechnology*, 2014, **25,** 445603 (1-6).
29 M. G. Moghaddam, R. H. Dabanlou, *J. of Industrial and Engineering Chemistry* 2014, 20, 739-744

